Journal of Composite Materials
http://jcm.sagepub.com/

Novel approach for mold filling simulation of the processing of natural fiber reinforced composites by resin transfer molding

Gastón Francucci, Exequiel S Rodríguez and Juan Morán

Journal of Composite Materials 2014 48: 191 originally published online 1 January 2013
DOI: 10.1177/0021998312469992

Article

JOURNAL OF COMPOSITE MATERIALS

Journal of Composite Materials
2014, Vol 48(2) 191–200

DOI: 10.1177/0021998312469992
jcm.sagepub.com
SAGE

Novel approach for mold filling simulation of the processing of natural fiber reinforced composites by resin transfer molding

Gastón Francucci, Exequiel S Rodríguez and Juan Morán

Abstract

Modeling the infiltration of reinforcements during the processing of composite materials by liquid composite molding techniques is an important instrument for the prediction of flow front patterns, filling times and pressure gradients. Darcy's law is widely used to model most of these processes. However, when polar fluids are used together with natural fibers, fiber swelling may occur and introduce further complexity to the simulation. In this work, a model that includes the aforementioned phenomena is proposed, leading to a more accurate prediction of the flow front position than the classic models that use a constant permeability value.

Keywords

Natural fiber composites, mold filling, finite element method, permeability, porosity

Introduction

Nowadays, great efforts are being made to reduce the environmental impact of materials and the dependence on nonrenewable resources. Therefore, new composites based on plant fibers and/or bio-resins are being produced. In most cases, these materials have low environmental impact since they are bio-degradable and/or they are produced from renewable resources. In addition, bio-resins and bio-fibers usually have economic advantages over petroleum-based materials.[1]

Liquid composite molding techniques such as resin transfer molding (RTM) and vacuum assisted resin transfer molding (VARTM) are suitable for processing these materials into complex shapes with a good surface quality on both sides of the part. In these techniques, a catalyzed resin is forced through a mold which contains the dry reinforcement. The reinforcement is impregnated by the resin during the infusion, and after curing, the part can be removed from the mold.

Nowadays, the manufacture process of a new component made by RTM begins usually in the computer, where the mold filling by the resin can be simulated. This allows predicting the filling time, the zones where air will be trapped, how the flow will workaround inserts and probably lead to unfilled regions, the presence of preferential paths for the resin flow, etc. Therefore, the design of the molds can be performed throughout computer simulations, modifying the geometry and location of vents, injection ports and resin distribution channels, until the result of the simulation is acceptable. This optimizes the process and reduces the production costs. As input parameters, these programs require the properties of the resin, such as the reaction kinetics and the evolution of viscosity with time and temperature. However, in most processes the resin cure is inhibited until the mold filling is complete, or activated afterwards by applying elevated temperatures, which makes the modeling of the process much easier as the resin viscosity can be considered to be constant. Some properties of the reinforcement

Composite Materials Group, Research Institute of Material Science and Technology (INTEMA-CONICET), Materials Engineering Department, Engineering Faculty, National University of Mar del Plata, Argentina

Corresponding author:
Juan Morán, Composite Materials Group, Research Institute of Material Science and Technology (INTEMA-CONICET), Materials Engineering Department, Engineering Faculty, National University of Mar del Plata, J. B. Justo 4302, B7608FDQ, Mar del Plata, Argentina.
Email: jmoran@fi.mdp.edu.ar

material are also needed as input parameters for the model, being the permeability of the preform the most relevant. Usually, the permeability is assumed to be constant for a particular reinforcing material, and it only depends on the fiber type, fabric architecture, and fiber volume fraction. Therefore, a model that relates the permeability of the preform with the fiber volume fraction is essential to predict the behavior of the resin flow during the processing of complex parts that present different thicknesses and/or fiber volume fractions. The modified Carman–Kozeny model can be used to establish a relationship between permeability and porosity (defined as: 1 - fiber volume fraction). The expression of the modified Carman–Kozeny model is shown in equation (1), where n and C are empirical parameters. The use of the exponent n other than 2, is not based on a flow mechanism and the model can be taken as an empirical model which fitted the experimental data as suggested by Francucci et al.,[2] Rodriguez et al.[3] and Shih and Lee.[4]

$$K = \frac{\varphi^{n+1}}{C(1-\varphi)^n} \tag{1}$$

Constitutive equations

Darcy's law is widely used to model the fluid flow through a porous medium, and it is also extensively used in modeling flow processes in composite materials manufacturing. This law is applicable when the flow occurs at low Reynolds numbers because inertial forces are neglected. In addition, the quasi-steady-state assumption should hold valid. This means that the saturation gradient developed at the flow front as a consequence of the delayed impregnation of the dense fiber tows with respect to the macroscopic flow front should be negligible.[5] This effect is caused by the difference in the local permeability of the inter-tow and intra-tow regions, and the capillary effects developed in the micro-pores inside the tows.

Darcy's law is shown in equation (2), where $\bar{u}$ is the averaged resin velocity (Darcy's velocity), K is the permeability tensor, η is the fluid viscosity and ∇P is the applied pressure gradient. Equation (3) shows the one-dimensional form of Darcy's law, taking into account that the Darcy's velocity is related to the superficial fluid velocity, v (which is the observable velocity $=\frac{\partial x_f}{\partial t}$, where x_f is the flow front position), through the porosity of the preform, φ.

$$\bar{u} = -\frac{\overline{\overline{K}}}{\eta}\nabla P \tag{2}$$

$$v = -\frac{K}{\varphi\eta}\frac{\partial P}{\partial x} \tag{3}$$

In addition, if no sinks or sources of fluid exist throughout the mold being filled, the continuity equation should be also used to describe the fluid flow. The expression for the one-dimensional continuity equation is

$$\frac{\partial}{\partial x}(\bar{u}_x) = 0 \tag{4}$$

Merging equations (2), (3) and (4) leads to

$$\frac{\partial}{\partial x}\left(\frac{K_{xx}}{\varphi\eta}\frac{\partial P}{\partial x}\right) = 0 \tag{5}$$

which means that the pressure distribution along the wetted region of the preform follows a linear behavior. The relationship between the pressure and the position of the flow front can be found if appropriate boundary conditions are established at the inlet and outlet resin ports.

Variable permeability of vegetable fiber fabrics

The modeling of the mold filling stage during the processing of composite materials by techniques such as resin transfer molding, vacuum assisted resin transfer molding, or vacuum infusion, has been studied by many authors. Several works can be found in literature showing different approaches and techniques used to achieve successful simulations. Usually, the modeling is based on the Darcy's law and the permeability of the reinforcement is considered to be constant.[6–10]

However, when natural fibers are used as reinforcement in RTM or VARTM processes, the permeability of the preform does not necessarily remain constant along the wetted region of the fabrics throughout the infiltration process. Many authors have probed that the permeability of natural fiber reinforcements decreases as the infiltration process takes place.[1,11–13] The main explanations for the experimental observations state that plant fibers absorb fluid from the main stream and then swell, decreasing the porosity of the preform as the open paths for flow are reduced. This effect adds a new issue to the modeling of the infiltration stage of the processing of natural fiber based composites: the variable permeability of the preform. The amount of fiber swelling and therefore, permeability variation, depends on the fiber-fluid system. In general, more polar fluids will enhance fiber swelling and will cause higher fabric permeability variations than less polar fluids.[14]

In the present work, a brief review on the current models developed to simulate the processing of natural

fiber reinforcements by RTM and/or VARTM is presented. In addition, novel procedures are proposed to model these processes. All the models proposed take into account the variation in permeability of the fabrics as the fibers absorb fluid and swell.

Materials and methods

Permeability tests

In order to verify the observations mentioned in the previous section, permeability tests were carried out on jute bidirectional woven fabrics (surface density equal to 0.03 g/cm^2). Two different test fluids were used: a nonpolar fluid, SAE 20 motor oil, which is not absorbed by the natural fibers; and a 25% V/V water/glycerin solution, which is a very polar fluid and causes fluid absorption and fiber swelling.[2] Prior to the permeability tests, the fabrics were washed with a 2% V/V distilled water and detergent solution, to remove contaminants and normalize the fabrics conditions for all the injections. Fibers were dried in an oven to remove humidity prior to the permeability tests. Unidirectional injection experiments were performed in a rectangular metallic mold (500 mm × 100 mm) with an acrylic lid. The depth of the mold cavity used for each injection was set by means of metallic spacers in order to obtain the desired values of preform's porosity. Mold deflection during the infiltration tests was avoided by using a 3 cm thick acrylic lid. Three injections were conducted for each porosity and type of fluid. The viscosity of the fluids used was measured before every infusion by means of a Brookfield DV–II + cone and plate viscometer. A vacuum pump was used to force the fluid flow though the mold cavity. The pressure gradient achieved was measured with a vacuum gauge, located at the outlet line of the mold. Unsaturated permeability values were obtained using Darcy's law expressed in the form of equation (6)

$$K_{unsat} = \frac{(\Phi \cdot m \cdot \mu)}{2\Delta P} \tag{6}$$

where K_{unsat} is the unsaturated permeability (m^2), m (m^2/s) is slope of the curve x^2 (square of the flow front position) versus time, μ is the fluid viscosity (Pa.s) and ΔP (Pa) is the pressure drop along the fiber bed. The relation between the flow front position and the injection time was obtained by recording the infusion process with a camera mounted on top of the transparent flow cell and a graduated grid printed on the acrylic surface.

Mold filling simulation

Masoodi and Pillai[14,15] have proposed different approaches to model the mold filling process when natural fibers are used as reinforcement. They obtained good results by assuming that the permeability of the wetted region of the preform to be a function of time exclusively. This means that the permeability value is uniform in the entire wetted part of the preform, and it changes with time as the injection proceeds. The authors proposed a linear relationship between the permeability of the wetted preform and time. Permeability tests were performed with a swelling and a nonswelling fluid to estimate the linear relationship parameters. Despite the simple relationship proposed between the permeability and time, the results obtained by the mentioned authors were acceptable, and they were more accurate than the ones obtained by neglecting the fluid absorption and fiber swelling effect on the permeability. Their model will be referred in this contribution as the homogeneously variable permeability model (HVPM).

Homogeneously variable permeability model. In this approach, the variation in the porosity of the preform as the fibers absorb fluid and swell is considered. Therefore, in this case, the permeability is assumed to remain constant for a given value of porosity and what changes is precisely the free space for fluid flow throughout the preform. The relation between the permeability and the time can be set by using the Carman–Kozeny model, and considering that the porosity is a function of time

$$K(t) = \frac{\varphi(t)^{n+1}}{C[1-\varphi(t)]^n} \tag{7}$$

In order to obtain the correct value of permeability at any given porosity of the preform, the model parameters, n and C, should be estimated from a permeability versus porosity curve. Permeability tests should be performed with a nonswelling fluid, such as the SAE 20 motor oil. The position of the flow front could then be predicted by solving equation (8)

$$\frac{\partial x_f}{\partial t} = \frac{\varphi(t)^n}{\eta C[1-\varphi(t)]^n}\frac{\delta P_{iny}}{x_f} \tag{8}$$

where δP_{iny} refers to the applied pressure gradient.

Then, in order to find $x_f(t)$ a mathematical expression that correlates the porosity of the preform with the immersion time in the fluid is needed. The change in

porosity with time can be calculated if the change in fiber diameter with time is known, as shown in equation (9), where φ_0 is the porosity of the dry preform and $D_f(t)/D_{f0}$ is the ratio between the instantaneous fiber diameter and the dry fiber diameter.

$$\varphi(t) = 1 - (1 - \varphi_0)\left(\frac{D_f(t)}{D_{f0}}\right)^2 \tag{9}$$

Curves showing the change in diameter of the fiber with the immersion time in the fluid can be obtained by performing swelling tests, in which the fibers are immersed in the test fluid and their diameter is monitored using an optical microscope and recorded at given periods of time with a digital camera.[2]

An exponential function is suitable for fitting the change in fiber diameter with time, as suggested by Masoodi and Pillai.[14] Such a function has three empirical parameters as shown in equation (10).

$$\frac{D_f(t)}{D_0} = a\exp\left(\frac{b}{c+t}\right) \tag{10}$$

The porosity of the preform as a function of time is given by equation (11), and the flow front position can be found using equation (12). It should be noted that this model considers that the entire wetted region of the reinforcement has the same porosity (or permeability) at every given time since the fluid reached the beginning of it.

$$\varphi(t) = 1 - (1 - \varphi_0)\left(a\exp\left(\frac{b}{c+t}\right)\right)^2 \tag{11}$$

$$x_f = \sqrt{\frac{2P_{iny}}{\eta C}\int \frac{\left\{1-(1-\varphi_0)\left[a\exp\left(\frac{b}{c+t}\right)\right]^2\right\}^n}{\left\{(1-\varphi_0)\left[a\exp\left(\frac{b}{c+t}\right)\right]^2\right\}^n}\mathrm{d}t} \tag{12}$$

The advantage of using this procedure is that only one permeability versus porosity curve is needed (the one obtained with the fluid that does not swell the fibers) to model the behavior of any fluid to be injected in the mold using any desired experimental condition. Then, swelling test should be done for each fluid in order to calculate the parameters a, b and c, but these tests are easier, cheaper and have less experimental complications than the permeability experiments. In addition, if the empirical parameters are calculated from permeability tests, the model might predict erroneously the flow front behavior if the real injection conditions differ from the ones using during the tests. This happens because the permeability tests could be finished before the fiber saturation time is reached, and therefore, the modeling of real injections that take longer filling times would not be considering the fiber saturation effect.

Permeability field model. The model presented in the previous section is easy to use and can be solved without implementing numerical methods. Despite it takes into account the change in fiber permeability (or porosity) as a consequence of fluid absorption and fiber swelling as the injection proceeds, it assumes that those properties are constant throughout the entire length of the wetted preform. This assumption could lead to a significant error in predicting the flow front position when bio-resins or polar fluids are used, because the porosity of the fully saturated zones (more distant from the flow front) can be very different of that of the unsaturated zones (closer to the front flow).

Therefore, a novel model called the permeability field model (PFM) is proposed in order to improve the flow behavior prediction when natural reinforcements are used. This model takes into account the fact that the zones of the wetted preform located more distant to the flow front remained immersed in the fluid longer than the zones of the wetted preform located closer to the front. This means that the degree of fiber swelling changes along the length of the wetted preform, leading to a field of porosities and permeabilities.

In this model, Darcy's law was used considering incompressible flow. The movement of the flow front was modeled with the technique called 'volume of fluid' (VOF), which uses the velocity field and a fully convective scheme with SUPG stabilization. Details of the technique can be seen elsewhere.[16,17]

In this method, a variable called α that determines the filling fraction of the domain is transported applying the material or substantial derivative (equation (13)). α equals to zero in the empty zones, and it is equal to one in the zones filled with fluid. The front flow location is established where $\alpha = 1/2$.

$$\frac{\mathrm{d}\alpha}{\mathrm{d}t} = \frac{\partial\alpha}{\partial t} + V\nabla\alpha = 0 \tag{13}$$

The material derivative is equal to zero, because no source or sink exist along the process domain.

The model was solved using the finite element method. The numerical scheme is performed in three steps. First, the pressure distribution, $P(x)$, is calculated over the entire domain. Then, the fluid velocity field, $V(x)$ is calculated from the previous obtained pressure field. Finally, the filling fraction, α, is advected by the local average values of the velocity field. The advection time is calculated for every step, and is chosen accordingly to keep the Courant number close to unity.

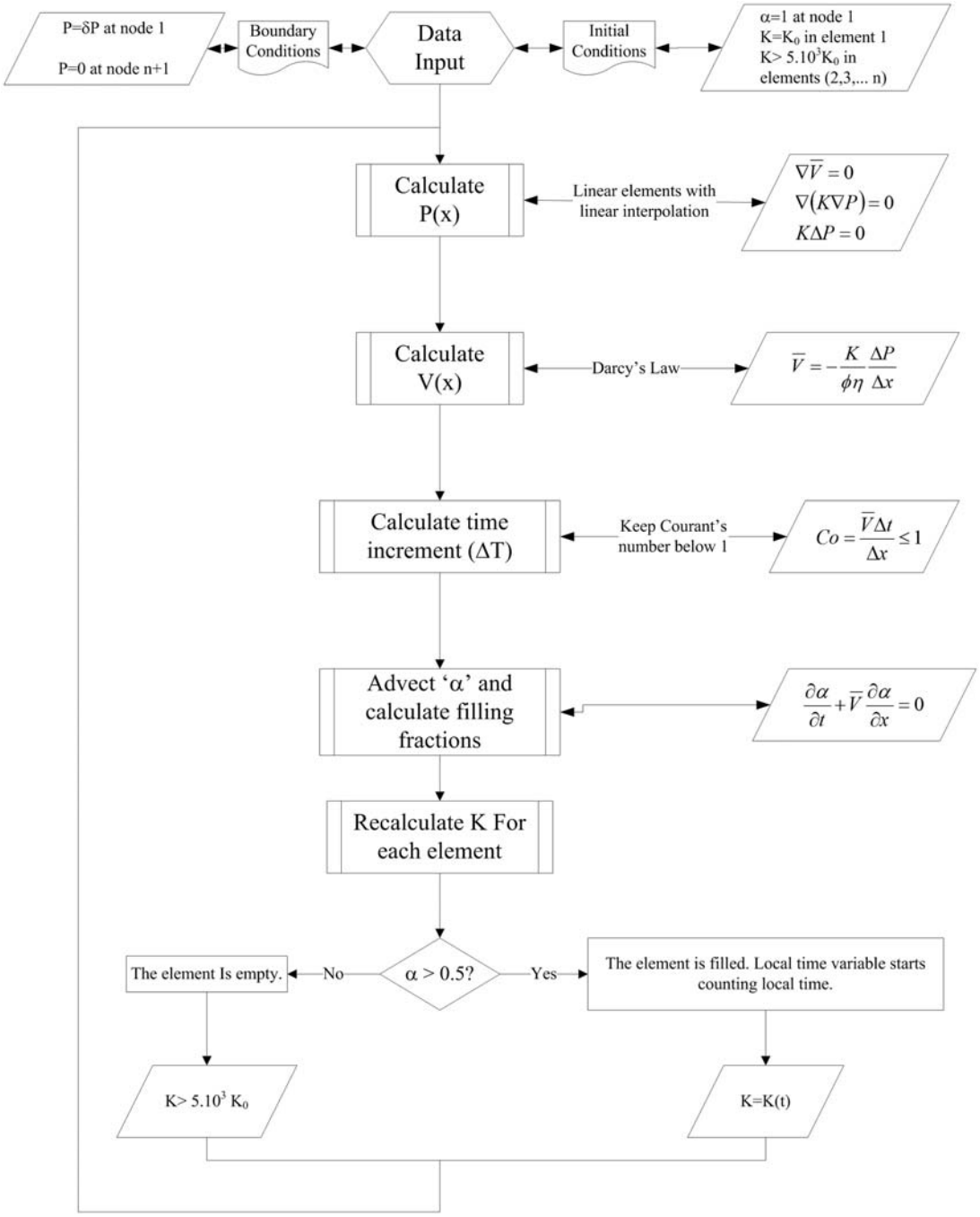

Figure 1. Solving scheme adopted.

Courant number is defined as the ratio of the length of propagation of a wave over a certain time increment divided by a characteristic element length. In this particular case $C_r = u_x{}^*\Delta t/\Delta x$. The time step is modified as the flow front advances, ensuring the algorithm stability. Figure 1 presents a flow chart showing the calculus algorithm.

Dirichlet boundary conditions were imposed at the nodes corresponding to the injection and vent points. At the injection point $P = \delta P$ while at the vent location $P = 0$, where δP is the relative injection pressure. Also, the permeability value in the wetted region of the preform ($\alpha > 1/2$) is $K(t)$ and it depends on the instantaneous porosity of each element of the mesh. The permeability in the dry region of the preform ($\alpha < 1/2$) is assumed to be 10^3–10^4 higher than the initial permeability, K_0 (the permeability calculated with a fluid that does not swell the fibers). By assigning to the dry

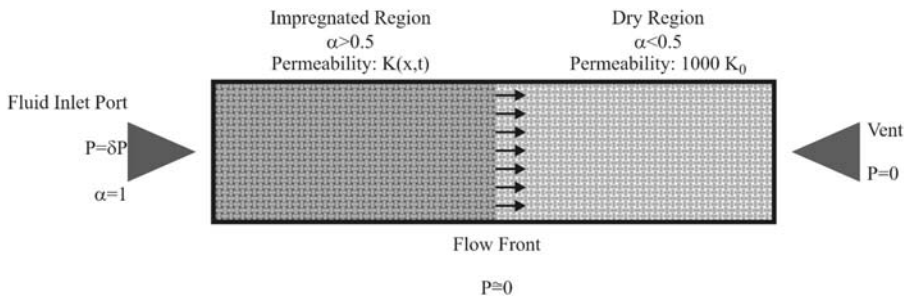

Figure 2. VOF technique scheme.
VOF: volume of fluid.

region of the preform a permeability value several times higher than to the wetted region allows to set a pressure value almost null at the front flow, without the need of setting boundary conditions to the moving front, making the algorithm more simple.

Every time a new element is 'filled' by the fluid ($\alpha > 1/2$), a local flag is raised by the program and a local 'element wetting time' starts to be computed by the algorithm. With this information, the algorithm calculates the porosity of each element in the domain by using equation (11), which empirical parameters should be calculated from swelling tests performed with the same fluid that is being modeled. The real permeability of each element can be obtained with the Carman–Kozeny model (equation (7)) by using the empirical parameters determined from the permeability curve obtained with a fluid that does not change the fiber diameter.

Figure 2 shows a scheme of the VOF technique to model the one-dimensional mold filling.

Results

Permeability results

Figure 3 shows the relationship between the unsaturated permeability of the fabrics and the porosity of the fiber bed obtained with the two different fluids. Experimental data was fitted with the modified Carman–Kozeny model for both test fluids, and the values of its parameters, n and C, are shown in Table 1.

As expected, the permeability of the fabrics measured with the polar fluid was lower than the permeability of the same fabrics measured with the nonpolar fluid, for the whole range of fiber volume fractions studied. This shows how fluid absorption and fiber swelling decreases the measured value of the permeability of natural fiber preforms. In addition, it can be seen in Figure 3 that the difference between both permeability curves is more important at higher porosities (lower fiber contents) because the amount of fiber swelling is higher when the porosity and the free space between fibers increase (free versus restricted swelling).

The permeability of any preform should be constant for a given value of porosity, no matter the fluid used to carry out the permeability tests (if the capillary effects are neglected). What happens in practice is that fiber swelling decreases the porosity of the preform when polar fluids are used, and therefore its permeability changes as the infiltration takes place, as found in a previous work.[2]

Mold filling simulations

In the permeability field model, each element of the mesh has its own permeability value, which is only a function of time (the entire element has the same permeability value at a given time). A permeability field along the wetted preform is generated because of the different immersion times experienced by each element. This implies that, despite the pressure drop is linear within each element, the global pressure distribution does not follow a linear behavior, as one would get from the models that consider a constant permeability value. Figure 4 shows the pressure curves for different flow front positions, obtained with the three models described in this contribution: the classic Darcy's law, HVPM, and PFM. The curves of the first two models were plotted with the same color because the pressure drop in both cases is linear and equal to $\Delta P/\Delta x$. On the other hand, the permeability field model predicts a higher pressure drop in the zones where the fibers experienced more swelling (further away from the flow front) than in the zones where fiber swelling was less significant (closer to the flow front).

The fluid velocity field predicted by the three models is shown in Figure 5. As expected, the models that take into account the decrease in porosity with time due to fiber swelling led to lower velocity curves tan the classic Darcy's law model. In addition, it can be seen that the velocity curves predicted by the models that consider fiber swelling diverge in a certain time range (between

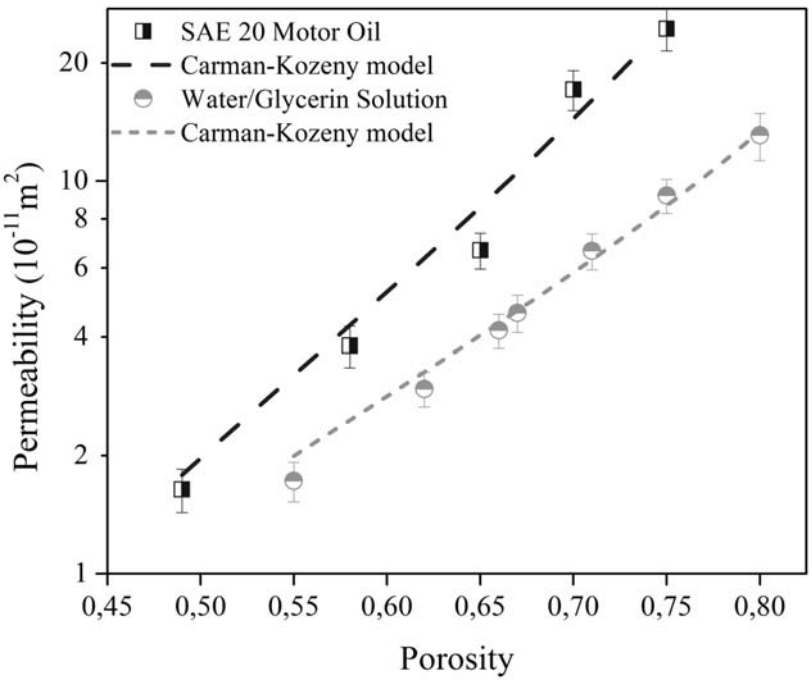

Figure 3. Permeability–porosity relationship for jute fiber preforms measured with apolar (water/glycerin solution) and a nonpolar fluid (SAE 20).

Table 1. Carman–Kozeny fitting parameters for the permeability–porosity curves.

	SAE 20 Motor oil	Water/Glycerin solution
n	1.954	1.289
C	2.538 E10	3.567 E10

180 and 2000 s). At the beginning of the injection (before 240 s) the fluid flows very rapidly and all the wetted preform stays immersed in the fluid approximately the same amount of time, and thus no significant differences can be seen between both models. At intermediate times the region of the wetted preform where a gradient of porosities exists is significant, and then both models predict a different fluid velocity (HVPM and PFM). The PFM predicts a higher flow rate than the HVPM, because the latter calculates the permeability of the entire wetted preform by using the time since the injection begins.

Therefore, the permeability predicted by the PFM is higher over a wider area of the wetted preform than the permeability predicted by the HVPM. Finally, after a long period of time (after 2200 s), the fluid flows very slowly, allowing the zones of the wetted preform closest to the flow front to reach the saturation porosity (the porosity when the fibers swell the maximum amount possible) and therefore the length over which the preform presents a porosity gradient is negligible with respect to the entire wetted preform. Consequently, the flow front velocities curves predicted by both models overlap at long injection times.

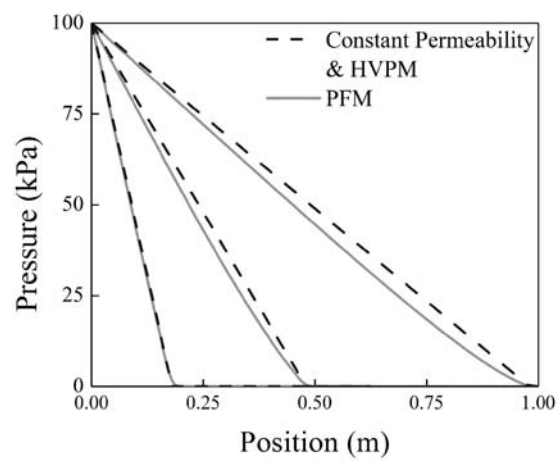

Figure 4. Pressure distribution predicted by the three models.

A scheme of the porosity variation in time predicted by the models is shown in Figure 6. In this scheme, the time range where the velocity curves separate is qualitatively indicated between t_1 and t_2. In addition, the fiber saturation time was also added to the scheme.

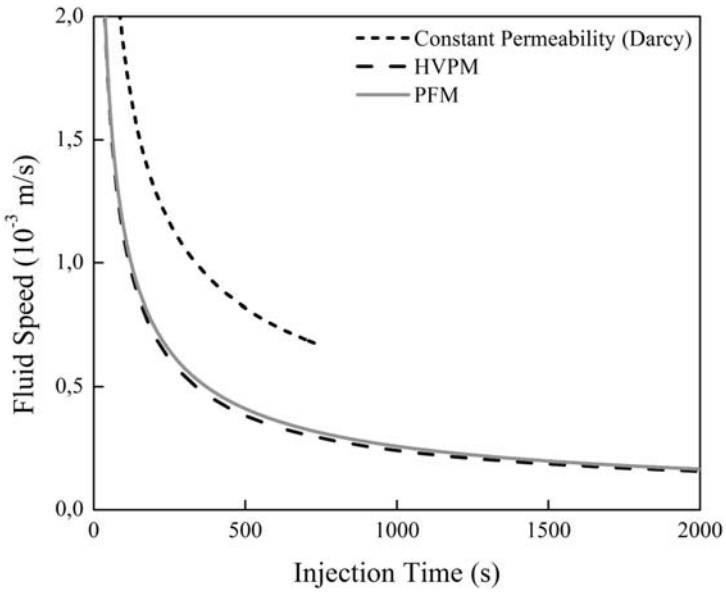

Figure 5. Evolution of the fluid velocity in time calculated by the three models.

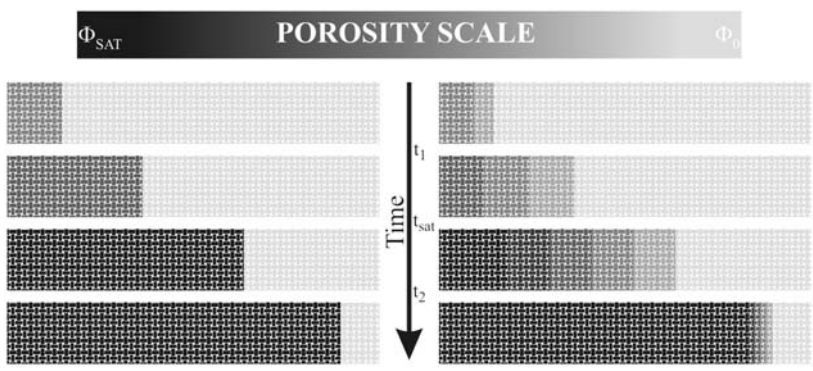

Figure 6. Variation in the porosity of the preform as the flow front advances: (a) HVPM; (b) PFM. HVPM: homogeneously variable permeability model; PFM: permeability field model.

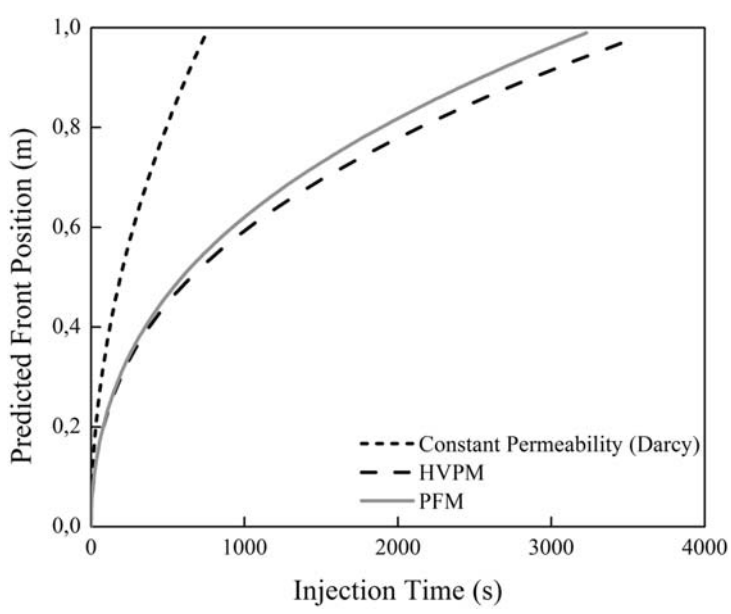

Figure 7. Predictions of the flow front position.

Despite the velocities predicted by both models are not significantly different, the small difference in velocity persists over a long period of time. Therefore, after the first stage in which no differences exist between the velocities calculated by each model, the prediction of the flow front movement is different, as shown in Figure 7. In addition, the difference between the flow front curves gets constant after the velocity curves calculated by both models overlap (after 2000 s approx.). As expected, Darcy's law (that considers permeability to be constant) predicts a faster mold filling that the models that consider fiber swelling. Table 2 presents the time required to fill a one-dimensional mold of one meter of length as estimated by the three models presented, with a 20% V/V water/glycerin solution and a dry porosity value $\varphi_0 = 0.7$. It can be seen that the permeability field model predicted a filling time 14% lower than the HVPM.

Table 2. Filling times for a 1 m long mold calculated with the three models.

Model	Filling time (min)
Constant permeability	12.5
HVPM	53.5
PFM	61

HVPM: homogeneously variable permeability model; PFM: permeability field model.

Figure 8 shows the flow front position versus time curves predicted by Darcy's law and the permeability field model, as well as the experimental data obtained from the video recordings taken during the permeability tests done with SAE 20 motor oil and the water/glycerin solution. It can be seen that the constant permeability model will not accurately predict the flow front movement when the water/glycerin solution is used in the test. On the other hand, the permeability field model showed a better fitting of the experimental data.

It should be noted that this novel model can be applied independently of the fluid used in the mold filling stage, since the parameters needed can be easily determined from the swelling tests for each fluid. If a nonswelling fluid is used, the permeability field model has the form of the Darcy's law, because $\varphi(t) = \varphi_0$ if $D_f(t)/D_{f0} = 1$ in equation (9).

Conclusions

In this work, two models were proposed to simulate the flow front movement during the one-dimensional RTM or VART processing of composite materials reinforced with natural fibers. This problem has been previously addressed by other authors; however, a different approach is presented. These models consider the effect of fluid absorption and fiber swelling on the porosity and permeability of the preform, which is not taken into account in classic models for synthetic fibers or in previous models for natural fibers processing.

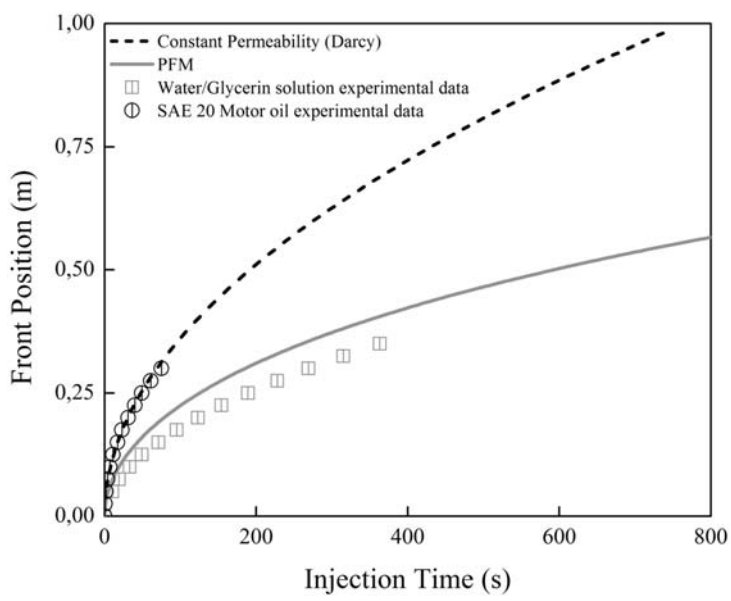

Figure 8. Experimental data fitting by the constant permeability model (Darcy's law) and the permeability field model.

The homogeneously variable permeability model, that was the first approach to model the process, considers that the permeability of the preform decreases with time due to fiber swelling, but the change in permeability is uniform throughout the entire wetted preform and is only a function of the injection time. On the other hand, the permeability field model, considers the fact that different regions of the wetted preform experience higher or lower fiber swelling depending on the amount of time that they have been immersed in the fluid. This leads to a field of permeability along the wetted fiber bed.

The results showed that all models that take into account the swelling of the fibers predict a much slower flow front movement that the model that assumes that permeability is constant over time. Comparing the two proposed models, the permeability field model predicts a greater flow rate than homogeneously variable permeability model, as expected, but this difference in the velocity field is small and occurs only during a certain time range. At the early stages of injection, the fluid flows so fast that the differences in immersion time and fiber swelling along the wetted preform are not significant. After the fluid has flowed a long distance from the inlet, the flow gets very slow, and the saturation gradient becomes very narrow and negligible with respect to the wetted preform length. Between these two mentioned events, the velocity curves predicted by the proposed models diverge. As a result, the flow front movement predicted by the permeability field model is faster, but this difference can be seen after the first stage of the injection, and remains constant even after the velocity curves predicted by both models overlap.

The experimental data was much better fitted by the permeability field model than by the constant permeability model when a swelling fluid was used in the permeability test.

Funding

The authors acknowledge the financial support provided by the National Research Council of Argentina (CONICET), as well as the SECYT (PICT 08-1628).

Conflict of interest

None declared.

References

1. Wool RP and Khot SN. *Bio-based resins and natural fibers*. Materials Park, Ohio: ASM International, 2001, pp.184–193.
2. Francucci G, Rodríguez ES and Vázquez A. Study of saturated and unsaturated permeability in natural fiber fabrics. *Compos Part A: Appl Sci Manuf* 2010; 41(1): 16–21.
3. Rodriguez E, Giacomelli F and Vazquez A. Permeability-porosity relationship in RTM for different fiberglass and natural reinforcements. *J Compos Mater* 2004; 38(3): 259–268.
4. Shih C-H and Lee LJ. Effect of fiber architecture on permeability in liquid composite molding. *Polym Compos* 1998; 19(5): 626–639.
5. Chan AW and Morgan RJ. Tow impregnation during resin transfer molding of bi-directional nonwoven fabrics. *Polym Compos* 1993; 14(4): 335–340.
6. Dungan FD and Sastry AM. Saturated and unsaturated polymer flows: microphenomena and modeling. *J Compos Mater* 2002; 36(13): 1581–1603.
7. Trochu F, Ruiz E, Achim V, et al. Advanced numerical simulation of liquid composite molding for process analysis and optimization. *Compos Part A: Appl Sci Manuf* 2006; 37(6): 890–902.
8. Michaud V and Mortensen A. Infiltration processing of fibre reinforced composites: governing phenomena. *Compos Part A: Appl Sci Manuf* 2001; 32(8): 981–996.
9. Liu X-L. Isothermal flow simulation of liquid composite molding. *Compos Part A: Appl Sci Manuf* 2000; 31(12): 1295–1302.
10. Joshi SC, Lam YC and Liu XL. Mass conservation in numerical simulation of resin flow. *Compos Part A: Appl Sci Manuf* 2000; 31(10): 1061–1068.
11. Umer R, Bickerton S and Fernyhough A. Characterising wood fibre mats as reinforcements for liquid composite moulding processes. *Compos Part A: Appl Sci Manuf* 2007; 38(2): 434–448.
12. Umer R, Bickerton S and Fernyhough A. Wood fiber mats as reinforcements for thermosets. In: Fakirov S and Bhattacharya D (eds) *Engineering biopolymers: homopolymers, blends and composites*. Munich: Hanser, 2007, pp.693–715.
13. Umer R, Bickerton S and Fernyhough A. Modelling the application of wood fibre reinforcements within liquid composite moulding processes. *Compos Part A: Appl Sci Manuf* 2008; 39(4): 624–639.
14. Masoodi R and Pillai KM. Modeling the processing of natural fiber composites made using liquid composite molding. In: Pilla S (ed.) *Handbook of bioplastics and biocomposites engineering applications*, New York: John Wiley & Sons, Inc., pp.43–73.
15. Masoodi R and Pillai KM. Darcy's law-based model for wicking in paper-like swelling porous media. *AIChE J* 2010; 56(9): 2257–2267.
16. Hirt CW and Nichols BD. Volume of fluid (VOF) method for the dynamics of free boundaries. *J Comput Phys* 1981; 39(1): 201–225.
17. Hughes TJR. *The finite element method: linear static and dynamic finite element analysis*. New York: Dover Publications, 2000.